Clim. Past Discuss., 2, 209–232, 2006
www.clim-past-discuss.net/2/209/2006/

Climate of the Past Discussions

Climate of the Past Discussions is the access reviewed discussion forum of *Climate of the Past*

Coupled climate model simulation of Holocene cooling events: solar forcing triggers oceanic feedback

H. Renssen[1], **H. Goosse**[2], **and R. Muscheler**[3]

[1]Faculty of Earth and Life Sciences, Vrije Universiteit Amsterdam, De Boelelaan 1085, 1081 HV Amsterdam, The Netherlands
[2]Institut d'Astronomie et de Géophysique G. Lemaître, Université Catholique de Louvain, 2 Chemin du Cyclotron, 1348 Louvain-la-Neuve, Belgium
[3]NASA/Goddard Space Flight Center, Climate & Radiation Branch, Greenbelt, MD 20771, USA

Received: 10 March 2006 – Accepted: 20 April 2006 – Published: 24 May 2006

Correspondence to: H. Renssen (hans.renssen@geo.falw.vu.nl)

Abstract

The coupled global atmosphere-ocean-vegetation model ECBilt-CLIO-VECODE is used to perform transient simulations of the last 9000 years, forced by variations in orbital parameters, atmospheric greenhouse gas concentrations and total solar irradiance (TSI). The objective is to study the impact of decadal-centennial scale TSI variations on Holocene climate variability. The simulations show that negative TSI anomalies can trigger temporary reorganizations in the ocean circulation that produce centennial-scale cooling events that are consistent with proxy evidence for Holocene cold phases. In the model, reduced solar irradiance leads to a relocation of the site with deepwater formation in the Nordic Seas, causing an expansion of sea ice that produces additional cooling. The consequence is a characteristic climatic anomaly pattern, with cooling over most of the North Atlantic region and drying in the tropics. Our results suggest that the oceans play an important role in amplifying centennial-scale climate variability.

1 Introduction

Centennial-scale climatic anomalies that occurred in the North Atlantic region during the last 11 500 years have been registered in a variety of paleoclimatic archives, such as marine sediments (e.g., Bond et al., 2001) , lake level data (e.g., Magny, 1993; Holzhauser et al., 2004) and glacier records (e.g., Denton and Karlén, 1973; Holzhauser et al., 2004). For instance, analyses of marine sediments have revealed the presence of enhanced concentrations of ice-rafted detritus (IRD) around 11.1, 10.3, 9.4, 8.1, 5.9, 4.2, 2.8, 1.4 and 0.4 ka BP, due to southward and eastward advection of cooler surface waters in the subpolar North Atlantic (Bond et al., 2001). The timing of these IRD events correlates with periods of reduced solar activity as reconstructed using cosmogenic isotopes (Bond et al., 2001), suggesting a confirmation of the solar-climate link proposed earlier by Denton and Karlén (1973) and Magny (1993) for cen-

tennial time-scale variability during the Holocene. This solar-climate link, however, has been debated because solar irradiance changes are assumed to be relatively small and probably cannot fully explain the temperature reductions (0.5 to 1°C in Europe, e.g., Luterbacher et al., 2004), suggesting that an amplifying mechanism is required to account for the magnitude of the observed climate changes (e.g., Rind, 2002).

Numerical climate models have been used extensively to study the impact of solar forcing on climate (e.g., Cubasch et al., 1997; Bertrand et al., 1999; Rind et al., 1999; Shindell et al., 2001), with most studies focusing on the well-known Maunder sunspot minimum (~1650–1700 AD, Eddy, 1976). Simulations performed by Shindell et al. (2001), for example, suggest that reduced total solar irradiance (TSI) during the Maunder Minimum could have resulted in changes in atmospheric circulation that enhanced the cooling over the Northern Hemisphere continents. In addition, several model studies have indicated that TSI variations could modify the behaviour of the oceanic circulation (e.g., Cubasch et al., 1997; Goosse et al., 2002; Weber et al., 2004).

Up to now, a realistic TSI reconstruction for the entire Holocene has not become available, thus hampering the execution of model studies to explore the solar-climate link on longer time-scales. However, recent analyses of the ^{14}C production rate and ice core ^{10}Be records (Muscheler et al., 2004a, 2005; Vonmoos et al., 2006[1]), now permits us to construct improved and more realistic estimates of TSI variations covering the last 9000 years. This has enabled us to perform transient simulations of the last 9000 years with a coupled climate model to study the impact of TSI variations on the Holocene climate. The objective of this paper is to investigate to what extent our model's response to these TSI variations can explain the centennial-scale Holocene cooling events registered in proxy records.

[1]Vonmoos, M., Beer, J., and Muscheler, R.: Large variations in Holocene solar activity – constraints from 10 Be in the GRIP ice core, Solar Physics, in revision, 2006.

2 Model and experimental design

We present results using the ECBilt-CLIO-VECODE global climate model, consisting of three main components describing the coupled atmosphere-ocean-vegetation system in three dimensions. The atmospheric component ECBilt is a quasi-geostrophic model with T21 horizontal and 3 levels (Opsteegh et al., 1998). ECBilt contains a full hydrological cycle, including a simple model for soil moisture over continents, and computes synoptic variability associated with weather patterns. Cloud cover is prescribed according to modern climatology. The oceanic component CLIO consists of a primitive-equation, free-surface ocean general circulation model (OGCM) coupled to a thermodynamic-dynamic sea-ice model (Goosse and Fichefet, 1999). The OGCM has a 3° latitude ×3° longitude resolution and 20 unevenly spaced levels, while the sea ice model has 3 layers. ECBilt-CLIO has been coupled to VECODE (Brovkin et al., 2002), a model that describes the dynamics of two vegetation types (grassland and forest) and a third dummy type (bare soil). The sensitivity to a doubling of atmospheric CO_2 concentration is 1.8°C, which is in the lower range of coupled climate models. Different versions of the model have successfully been used for simulation studies on a variety of topics, including the impact of freshwater perturbations (Renssen et al., 2001; 2002; Wiersma and Renssen, 2006), solar forcing of climate change (Goosse et al., 2002; van der Schrier et al., 2002; Goosse and Renssen, 2004; Weber et al., 2004), the climate of the last millennium (Goosse et al., 2004; Goosse et al., 2005a; b) and future climate evolution (Schaeffer et al., 2002, 2005). Further details about the ECBilt-CLIO-VECODE model are available at http://www.knmi.nl/onderzk/CKO/ecbilt.html.

We performed a 5-member ensemble simulation forced by time-varying forcings for the last 9000 years: orbital forcing (Berger, 1978), atmospheric trace gas concentrations (Raynaud et al., 2000) and TSI variations (Figs. 1a–d). The applied orbital and greenhouse gas forcing is identical to that used by Renssen et al. (2005a, b), while the TSI forcing time-series were newly constructed for this study. The ensemble members differ only in their initial conditions, which were derived from a multimillennial equilib-

rium experiment with constant forcings for 9000 BP.

TSI variations are prescribed as an anomaly of the solar constant (maximum negative anomaly is $-3.4\,\mathrm{Wm}^{-2}$) and are based on the ^{14}C production rate derived from the tree-ring Δ^{14}C record (Stuiver et al., 1998; Muscheler et al., 2005). To correct for the non-linear relationship between solar magnetic shielding, geomagnetic dipole field intensity and ^{14}C production rate we used model results (Masarik and Beer, 1999) to infer the solar modulation parameter that parameterises the galactic cosmic ray deflection due to the solar wind. The ^{14}C production rate was reconstructed under the assumption of a constant carbon cycle (Muscheler et al., 2005). Especially on the decadal to centennial time scales, which are of interest in our analysis, the potential for carbon cycle induced changes in Δ^{14}C is not very large (Muscheler et al., 2004b). In addition, the agreement between ^{14}C production rate and ^{10}Be measured in ice cores on these time scales gives us confidence that we are able to isolate the production signal induced by the variable sun (Muscheler et al., 2004a; Vonmoos et al., 2006[1]). On millennial time scales, however, potential changes in solar activity are not well constrained. ^{10}Be from Summit, Greenland, indicates different long-term changes compared to the ^{14}C production rate (Muscheler et al., 2005; Vonmoos et al., 2006[1]). This might be due to changes in the carbon cycle or in the atmospheric ^{10}Be transport and deposition onto ice sheets. In addition, within the relatively large uncertainties of the geomagnetic field reconstructions (Yang et al., 2000; Muscheler et al., 2005), the long-term changes in the ^{14}C production rate can be explained by geomagnetic field changes. Therefore, due to the uncertainties connected to the data, long-term changes in solar activity cannot be yet inferred with this method. To avoid introducing an artificial trend in our solar forcing record, we removed the long-term trend in the solar modulation parameter by subtracting a 5th order polynomial fitted to the data.

To obtain TSI variations we assumed that the solar modulation parameter scales linearly to the variations in total solar irradiance. Maunder minimum type solar minima are assumed to represent a TSI reduction of $2.6\,\mathrm{Wm}^{-2}$ based on Lean (2000). The last two assumptions introduce the largest uncertainties in our irradiance record. However,

due to lack of precise knowledge of long-term TSI changes we think that this record is a first and reasonable step to quantitatively study the solar influence on climate on longer time scales. To reduce the short-term noise in the forcing TSI series, we applied a 55-yr running mean filter (Fig. 1c).

3 Results and discussion

3.1 Global climate response to TSI variations

The ensemble-mean result for the global surface temperature (Fig. 2a) represents the system's forced response, as the averaging suppresses the internal variability (e.g., Goosse et al., 2005). The simulated ensemble-mean long-term cooling trend in annual global surface temperature (from 15.95°C to 15.65°C) is associated with the orbital forcing. Earlier experiments with the same model showed that the millennial-scale annual temperature evolution closely follows the decreasing orbitally-forced insolation trends in particular seasons, i.e., June–July in the Northern Hemisphere (Renssen et al., 2005a) and September–October in the Southern Hemisphere (Renssen et al., 2005b). Decadal-to-centennial scale variations, on the other hand, are primarily controlled by TSI anomalies at this time-scale (r is 0.76 after removal of the large-scale cooling trend). For individual ensemble members this relationship is less straightforward (r is 0.31) due to the system's internal variability.

Previous sensitivity experiments (Goosse et al., 2002; Goosse and Renssen, 2004) performed with ECBILT-CLIO focused at TSI anomalies revealed that reductions in radiative forcing could potentially trigger a local temporary shutdown of deep convection in the Nordic Seas (i.e., South of Svalbard). In our model, such local convection failures could take place as part of a low-frequency mode of internal variability (i.e., they also occur without external forcing, Goosse et al., 2002), a phenomenon described in at least one other coupled climate model (Hall and Stouffer, 2001). These events are linked to sea-ice expansion during relatively cold phases, which stratifies the water

column and hampers deep convection. In experiments with constant preindustrial forcing (Goosse and Renssen, 2004), the probability for having a year with such a local convection failure is 0.04.

In our ensemble experiment with variable solar forcing this probability is slightly higher (0.07) when calculated for the entire 9000 year-period, while it varies between 0 and 0.19 when computed for 50-year periods (Fig.2b). Most of the higher values (>0.14) are associated with TSI minima (7 out of 8). Particularly during the last 4500 years, all major negative TSI anomalies (less than $-2\,\mathrm{Wm}^{-2}$ or >2 standard deviations) are followed by high probability values within 100 years, i.e., centered at 4.3, 3.8, 3.2, 2.6, 2.3, 1.3, 0.9, 0.7 and 0.4 ka BP. It is important to note that a probability maximum does not necessarily imply a local convection shut-down in all ensemble members. Rather, it suggests that the probability of a convection failure in the Nordic Seas was significantly higher after large TSI anomalies than without a reduction in radiative forcing (Goosse and Renssen, 2004). In the first 4500 years of our experiments, the probability is generally lower than in the second half of the simulations. The early Holocene climate in the Arctic is relatively warm as a consequence of the high orbitally-forced summer insolation values, leading to reduced sea-ice cover and less interference with deep convection (Renssen et al., 2005a).

3.2 The simulated climate response during 3000–2000 BP

The impact of solar forcing on deep convection and the surface climate can be illustrated in detail using the 3000–2000 BP period, which includes two marked negative TSI anomalies centred at 2700 BP and 2300 BP (Fig. 3a). For this period we performed four additional 1500-year long experiments that differ in initial conditions (started at 3500 BP). In general, the global atmospheric temperature closely follows the TSI anomaly. During the period with lowest TSI values (2730–2700 BP), generally cooling occurs around the globe, with strongest cooling (up to 0.5°C in the ensemble mean) over Northern Hemisphere (NH) mid-latitude continents (Fig. 4a), while the temperature reduction over the oceans is relatively small (generally <0.1°C) due to the

ocean's large heat capacity. In the Nordic Seas region a characteristic temperature anomaly pattern is visible with enhanced cooling (more than −0.6°C) South of Svalbard and warming (0.4°C) near Iceland, associated with a shift in deep water formation from the former to the latter location. After the lowest TSI values at 2700 BP, the global surface temperature and TSI diverge. Between 2650 and 2600 BP, when the TSI values have increased again, temperatures remain relatively low (Fig. 3a). This could be partly attributed to the thermal inertia of the oceans, causing the ocean temperatures and sea-ice cover to lag solar forcing. However, in addition, the cooling has resulted in considerable build-up of Arctic sea-ice (Fig. 3b) that sustains the local deep convection shutdown South of Svalbard, causing an amplified cooling over the eastern Nordic Seas and Barents Sea (Fig. 4b). In 2 (out of 9) ensemble members, this shift in convection location is accompanied by important reductions in the strength of the meridional overturning circulation (MOC) in the Nordic Seas (from 3.0 Sv to 2.5 Sv). Likewise, the maximum cooling in individual ensemble members can be substantially larger than the ensemble mean (i.e., up to 1°C in Europe, Fig. 4c).

The global atmospheric temperature response to the second negative TSI anomaly centred at 2300 BP is more direct and shows no lag as observed after 2700 BP (Fig. 3a). This is related to the shorter duration of this TSI anomaly and to the relatively high TSI values before and after the negative excursion. In all ensemble members a temporary local convection-shutdown is simulated around 2300 BP similar to 2700 BP, but the TSI anomaly centred at 2300 BP is too short for extensive sea-ice build-up that extends the cooling (Fig. 3b). Indeed, in our ensemble experiment, significant extension of the cooling event is only seen after a few relatively long-lasting TSI anomalies (i.e., at 5.2, 2.7 and 0.5 ka BP).

Associated with major negative TSI anomalies, also a characteristic pattern in precipitation is simulated, with a marked drying over the Northern Africa (Fig. 5) caused by weakened summer monsoons, related to a stronger continental cooling compared to the tropical oceans. Here, the precipitation is reduced by more than 10% (or 20–40 mm) on an annual basis. Precipitation anomalies elsewhere are relatively small and

statistically insignificant.

3.3 Comparison with proxy evidence for the 2800–2600 BP event

When comparing proxy data with our model results, it is important to realise that reality represents only one out of many possible realizations of the climate system. Consequently, when comparing model results for the 2800–2600 BP event with proxy data, we should not look at the ensemble mean. Rather, if model and data are consistent, one would expect that the proxy signal lies within the simulated climate range of the ensemble set (c.f., Goosse et al., 2005b; 2006). In this respect, the climatic signal registered in proxies is analogous to results of a particular ensemble member. In our experiments, the ensemble member that is closest to these data is the coldest ensemble member (Fig. 4c).

Most simulated climate anomalies for the 2800–2600 BP event are consistent with proxy evidence (Table 1). North Atlantic marine records show a marked surface cooling, particularly in the Norwegian Sea (Mikalsen et al., 2001; Andersson et al., 2003; Risebrobakken et al., 2003) where the anomaly reached −1.5°C, which is a bit colder than our coldest ensemble member (Fig. 4c). Moreover, the cold surface waters in the North Atlantic (Fig. 4c) favour the southward advection of drift ice transporting IRD (Bond et al., 2001). Deep ocean records strongly suggest that the surface cooling is accompanied by a distinct reduction in MOC strength (Bianchi and McCave, 1999; Oppo et al., 2003; Hall et al., 2004). In Europe the 2800–2600 BP period was a widespread cool phase, with dry conditions in Norway (Nesje et al., 2001), but relatively wet conditions in Western Europe (e.g., Magny, 1993; van Geel et al., 1996; 1998; Macklin et al., 2003; Holzhauser et al., 2004). In Eastern North America (New England and Michigan) also proxy evidence is found for anomalous wet conditions aound 2800–2600 BP (Brown et al., 2000; Booth and Jackson, 2003). The increases in precipitation at NH mid-latitudes in our simulation results (Fig. 5) are very small and not statistically significant.

The simulated warming near Iceland agrees with some records indicating that the

North Icelandic shelf experienced a warm inflow (e.g., Giraudeau et al., 2004; Andersen et al. 2004) starting at 2800 BP. Other marine records from this region indicate first a cold phase, followed by a warming (Jiang et al., 2002). Because of the local warming near Iceland, there is no clear cooling signal over Greenland in our model, which is consistent with the reconstructed stable site temperature for the Greenland ice cores (Masson-Delmotte et al., 2005). However, analysis of variations in chemical species in the GISP2 ice core that reflect changes in atmospheric circulation (i.e., a regional signal) have revealed anomalous cold and windy conditions in the period 2800–2600 BP (O'Brien et al., 1995). Over Northwestern Africa, a marked dry event is recorded in various types of data (van Geel et al., 1998; Elenga et al., 2004) in agreement with our simulation.

In summary, proxy data show that the 2800–2600 BP is characterised by widespread cooling (especially in the North Atlantic region), reduced MOC strength, wet conditions over NH mid-latitude continents and dry conditions over Northern Africa. Proxy archives show a very similar climate anomaly around 5300 BP (Magny and Haas, 2004), i.e. the timing of a major TSI minimum and extended cool phase in our simulations. Our results show many similarities to this characteristic pattern, suggesting that centennial-scale Holocene cooling events could be an expression of the combined effect of solar forcing and the discussed positive oceanic feedback, indicating a larger role for the oceans in driving centennial-scale climate changes than recognized until now. Our simulation results suggest that the probability of a local deep convection failure in the Nordic Seas increases in periods following a major negative TSI anomaly. Consequently, in the real world not all TSI reductions should necessarily have resulted in such a local convection shut-down and conversely, these convection failures could also have occurred without relatively low TSI values in the preceding period. The stochastic nature of the discussed oceanic feedback could thus explain why the correlation between reconstructed TSI and climate reconstructions is generally lower on decadal-centennial timescales than might be expected in the case of a direct linear solar-climate link.

Previous studies have suggested that the amplifying factor behind Holocene cooling

events involves a stratospheric response to TSI reductions (Haigh, 1994, 1996; van Geel et al., 1998, 2000; van Geel and Renssen, 1998). This was based on model studies (Haigh, 1994, 1996) indicating that during negative TSI anomalies the relatively large reduction in incoming UV radiation caused decreases in lower stratospheric ozone formation, resulting in amplified stratospheric cooling and a change in circulation that could propagate downward. In the troposphere, this could lead to contraction of the Hadley Cells and expansion of the polar cells, resulting in drier conditions in the tropics and cooling at mid-latitudes (Haigh, 1994; van Geel et al., 1998). Our model does not include this mechanism as it lacks a dynamical stratosphere. Consequently, in our simulations the cool mid-latitudes and dry tropics cannot be attributed to this stratospheric mechanism. However, as mentioned, TSI reconstructions extending the period of direct satellite-based observation contain an uncertainty so that it is unclear by how much TSI was reduced during periods such as the Maunder minimum. Our estimate is probably at the upper limit of realistic estimates (e.g., Wang et al., 2005) of the changes from periods with almost no sunspots to periods of relatively high solar activity. Changes in ozone and energy absorption in the stratosphere due to the variable sun, however, could amplify the direct solar forcing and act in a similar way, also resulting in a displacement the location of deep convection. Therefore, in future climate modelling studies considering the impact of TSI variations on the Holocene climate, the effect of stratospheric ozone should ideally be accounted for.

4 Conclusions

We have presented transient experiments performed with a coupled climate model to investigate the impact of TSI variations on decadal-centennial scale climate variability during the last 9000 years. Our results suggest the following.

1. In our model, negative TSI anomalies increase the probability of a local shutdown of deep convection in the Nordic Seas. The initial cooling associated with TSI reductions leads to sea-ice expansion in the area, which stratifies the water column and hampers deepwater formation, leading to additional cooling and more sea-ice. This positive oceanic feedback amplifies the solar-forced cooling in the North Atlantic region, while in the tropics the climate becomes drier.
2. In the first 4500 years of our simulation, the probability to have a local convection failure in the Nordic Seas is smaller than during the second half of our simulations. This is related to the relatively warm early Holocene climate at high northern latitudes, which is due to the relatively high orbitally-forced summer insolation at that time.
3. Following relatively long-lasting negative TSI anomalies (centered at 5.2, 2.7 and 0.5 ka BP), extensive sea-ice buildup results in extension of the cooling event by about 50 years.
4. The characteristic climatic anomalies for simulated events centered around 5.2 and 2 ka BP are consistent with proxy evidence, suggesting that the positive oceanic feedback has played an important role in driving Holocene cooling events.

Acknowledgements. H. Renssen is supported by the Netherlands Organization for Scientific Research (N.W.O). H. Goosse is Research Associate with the Fonds National de la Recherche Scientifique (Belgium) and is supported by the Belgian Federal Science Policy Office. R. Muscheler was supported by the Swiss Science Foundation.

References

Andersen, C., Koç, N., Jennings, J., and Andrews, J. T.: Nonuniform response of the major surface currents in the Nordic Seas to insolation forcing: implications for the Holocene climate variability, Paleoceanography, 19, PA2003, doi:10.1029/2002PA000873, 2004.

Andersson, C., Risebrobakken, B., Jansen, E., and Dahl, S. O.: Late Holocene surface ocean conditions of the Norwegian Sea (Vøring Plateau), Paleoceanography, 18, 1044, doi:10.1029/2001PA000654, 2003.

Berger, A. L.: Long-term variations of daily insolation and Quaternary climatic changes, J. Atmos. Sci., 35, 2363–2367, 1978.
Bertrand, C., van Ypersele, J.-P., and Berger, A.: Volcanic and solar impacts on climate since 1700, Clim. Dyn., 15, 355–367, 1999.
Bianchi, G. G. and McCave, I. N.: Holocene periodicity in North Atlantic climate and deep-ocean flow south of Iceland, Nature, 397, 515–517, 1999.
Bond, G., Showers, W., Cheseby, M., Lotti, R., Almasi, P., deMenocal, P., Priore, P., Cullen, H., Hajdas, I., and Bonani, G.: A pervasive millennial-scale cycle in North Atlantic Holocene and Glacial climates, Science, 278, 1257–1266, 1997.
Bond, G. C., Showers, W., Elliot, M., Evans, M., Lotti, R., Hajdas, I., Bonani, G., and Johnsen, S.: The North Atlantic's 1–2 kyr climate rhythm: relation to Heinrich events, Dansgaard/Oeschger cycles and the Little Ice Age, AGU Geophysical Monograph, 112, 35–58, 1999.
Bond, G. C., Kromer, B., Beer, J., Muscheler, R., Evans, M. N., Showers, W., Hoffmann, S., Lotti-Bond, R., Hajdas, I., and Bonani, G.: Persistent solar influence on North Atlantic climate during the Holocene, Science, 294, 2130–2133, 2001.
Booth, R. K. and Jackson, S. T.: A high-resolution record of late-Holocene moisture availability from a Michigan raised bog, USA, Holocene, 13, 863–876, 2003.
Brovkin, V., Bendtsen, J., Claussen, M., Ganopolski, A., Kubatzki, C., Petoukhov, V., and Andreev, A.: Carbon cycle, vegetation and climate dynamics in the Holocene: experiments with the CLIMBER-2 model, Global Biogeochem. Cycles, 16, doi:10.1029/2001GB001662, 2002.
Brown, S. L., Bierman, P. R., Lini, A., and Southon, J.: 10 000 yr record of extreme hydrological events, Geology, 28, 335–338, 2000.
Cubasch, U., Voss, R., Hegerl, G. C., Waszkewitz, J., and Crowley, T. J.: Simulation of the influence of solar radiation variations on the global climate with an ocean-atmosphere general circulation model, Clim. Dyn., 13, 757–767, 1997.
Denton, G. H. and Karlén, W.: Holocene climatic variations – Their pattern and possible causes, Quat. Res., 3, 155–205, 1973.
Eddy, J. A.: The Maunder minimum, Science, 192, 1189—202, 1976.
Elenga, H., Maley, J., Vincens, A., and Farrera, I.: Palaeoenvironments, palaeoclimates and landscape development in Atlantic Equatorial Africa: a review of key sites covering the last 25 kyrs, in: Past climate variability through Europe and Afrcia, edited by: Battarbee, R. W.,

Gasse, F., and Stickley, C. E., Springer, Dordrecht, 181–198, 2004.
Giraudeau, J., Jennings, A. E., and Andrews, J. T.: Timing and mechanisms of surface and intermediate water circulation changes in the Nordic Seas over the last 10 000 cal years: a view from the North Iceland shelf, Quat. Sci. Rev., 23, 2127–2139, 2004.
Goosse, H. and Fichefet, T.: Importance of ice-ocean interactions for the global ocean circulation: a model study, J. Geophys. Res., 104, 23 337–23 355, 1999.
Goosse, H. and Renssen, H.: Exciting natural modes of variability by solar and volcanic forcing: idealized and realistic experiments, Clim. Dyn., 23, 153–163, 2004.
Goosse, H., Renssen, H., Selten, F. M., Haarsma, R. J., and Opsteegh, J. D.: Potential causes of abrupt climate events: a numerical study with a three-dimensional climate model, Geophys. Res. Lett., 29, 1860, doi:10.1029/2002GL014993, 2002.
Goosse, H., Masson-Delmotte, V., Renssen, H., Delmotte, M., Fichefet, T., Morgan, V., van Ommen, T., Khim, B. K., and Stenni, B.: A late medieval warm period in the Southern Ocean as a delayed response to external forcing?, Geophys. Res. Lett., 31, L06203, doi:10.1029/2003GL019140, 2004.
Goosse, H., Crowley, T. J., Zorita, E., Ammann, C. M., Renssen, H., and Driesschaert, E.: Modelling the climate of the last millennium: what causes the differences between simulations?, Geophys. Res. Lett., 32, L06710, doi:10.1029/2005GL022368, 2005a.
Goosse, H., Renssen, H., Timmermann, A., and Bradley, R. S.: Internal and forced climate variability during the last millennium: A model-data comparison using ensemble simulations, Quat. Sci. Rev., 24, 1345–1360, 2005b.
Goosse, H., Renssen, H., Timmermann, A., Bradley, R. S., and Mann, M. E.: Using paleoclimate proxy-data to select optimal realisations in an ensemble of simulations of the past millennium, Clim. Dyn., doi:10.1007/s00382-006-0128-6, 2006.
Haigh, J. D.: The role of stratospheric ozone in modulating the solar radiative forcing of climate, Nature, 370, 544–546, 1994.
Haigh, J. D.: The impact of solar variability on climate, Science, 272, 981–984, 1996.
Hall, A. and Stouffer, R. J.: An abrupt climate event in a coupled ocean-atmosphere simulation without external forcing, Nature, 409, 171–174, 2001.
Hall, I. R., Bianchi, G. G., and Evans, J. R.: Centennial to millennial scale Holocene climate-deep water linkage in the North Atlantic, Quat. Sci. Rev., 23, 1529–1536, 2004.

Holzhauser, H., Magny, M., and Zumbühl, H. J.: Glacier and lake-level variations on west-central Europe over the last 3500 years, Holocene, 15, 789–801, 2005.

Jiang, H., Seidenkrantz, M. S., Knudsen, K. L., and Eiriksson, J.: Late-Holocene summer sea-surface temperatures based on a diatom record from the north Icelandic shelf, Holocene, 12, 137–147, 2002.

Lean, J.: Evolution of the Sun's Spectral Irradiance Since the Maunder Minimum, Geophys. Res. Lett., 27, 2425–2428, 2000.

Luterbacher, J., Dietrich, D., Xoplaki, E., Grosjean, M., and Wanner, H.: European seasonal and annual temperature variability, trends and extremes since 1500 AD, Science, 303, 1499–1503, 2004.

Macklin, M. G., Johnstone, E., and Lewin, J.: Pervasive and long-term forcing of Holocene river instability and flooding in Great Britain by centennial-sclae climate change, Holocene, 15, 937–943, 2003.

Magny, M. and Haas, J. N.: A major widespread climatic change around 5300 cal. yr BP at the time of the Alpine Iceman, J. Quat. Sci., 19, 423–430, 2004.

Magny, M.: Solar influences on Holocene climatic changes illustrated by correlations between past lake-level fluctuations and the atmospheric ^{14}C record, Quat. Res., 40, 1–9, 1993.

Masarik, J. and Beer, J.: Simulation of particle fluxes and cosmogenic nuclide production in the Earth's atmosphere, J. Geophys. Res., 104, 12 099–12 111, 1999.

Masson-Delmotte, V., Landais, A., Stievenard, M., Cattani, O., Falourd, S., Jouzel, J., Johnsen, S. J., Dahl-Jensen, D., Sveinsbjorndottir, A., White, J. W. C., Popp, T., and Fischer, H.: Holocene climatic changes in Greenland: different deuterium excess signals at Greenland ice core project (GRIP) and NorthGRIP, J. Geophys. Res., 110, D14102, doi:10.1029/2004JD005575, 2005.

Mikalsen, G., Sejrup, H. P., and Aarseth, I.: Late-Holocene changes in ocean circulation and climate: foraminiferal and isotopic evidence from Sulafjord, western Norway, Holocene, 11, 437–446, 2001.

Muscheler, R., Beer, J., Wagner, G., Laj, C., Kissel, C., Raisbeck, G. M., Yiou, F., and Kubik, P. W.: Changes in the carbon cycle during the last deglaciation as indicated by the comparison of ^{10}Be and ^{14}C records, Earth Planet. Sci. Lett., 219, 325–340, 2004a.

Muscheler, R., Beer, J., and Vonmoos, M.: Causes and timing of the 8200 y BP event inferred from the comparison of the GRIP ^{10}Be and the tree ring Δ^{14}C record, Quat. Sci. Rev., 23, 2105–2115, 2004b.

Muscheler, R., Beer, J., Kubik, P. W., and Synal, H.-A.: Geomagnetic field intensity during the last 60 000 years based on ^{10}Be & ^{36}Cl from the Summit ice cores and ^{14}C, Quat. Sci. Rev., 24, 1849–1860, 2005.

Nesje, A., Matthews, J. A., Dahl, S. O., Berrisford, M. S., and Andersson, C.: Holocene glacier fluctuations of Flatebreen and winter-precipitation changes in the Jostedalsbreen, western Norway, based on glaciolacustrine sediment records, Holocene, 11, 267–280, 2001.

O'Brien, S. R., Mayewski, P. A., Meeker, L. D., Meese, D. A., Twickler, M. S., and Whitlow, S. I.: Complexity of Holocene climate as reconstructed from a Greenland ice core, Science, 270, 1962–1964, 1995.

Oppo, D. W., McManus, J. F., and Cullen, J. L.: Deepwater variability in the Holocene epoch, Nature, 422, 277–278, 2003.

Opsteegh, J. D., Haarsma, R. J., Selten, F. M., and Kattenberg, A.: ECBILT: A dynamic alternative to mixed boundary conditions in ocean models, Tellus, 50A, 348–367, 1998.

Raynaud, D., Barnola, J.-M., Chappellaz, J., Blunier, T., Indermühle, A., and Stauffer, B.: The ice record of greenhouse gases: a view in the context of future changes, Quat. Sci. Rev., 19, 9–17, 2000.

Renssen, H., Goosse, H., Fichefet, T., and Campin, J.-M.: The 8.2 kyr BP event simulated by a global atmosphere-sea-ice-ocean model, Geophys. Res. Lett., 28, 567–570, 2001.

Renssen, H., Goosse, H., and Fichefet, T.: Modeling the effect of freshwater pulses on the early Holocene climate: the influence of high frequency climate variability, Paleoceanography, 17, 1020, doi:10.1029/2001PA000649, 2002.

Renssen, H., Goosse, H., Fichefet, T., Brovkin, V., Driesschaert, E., and Wolk, F.: Simulating the Holocene climate evolution at northern high latitudes using a coupled atmosphere-sea ice-ocean-vegetation model, Clim. Dyn., 24, 23–43, 2005a.

Renssen, H., Goosse, H., Fichefet, T., Masson-Delmotte, V., and Koç, N.: The Holocene climate evolution in the high-latitude Southern Hemisphere simulated by a coupled atmosphere-sea ice-ocean-vegetation model, Holocene, 15, 951–964, 2005b.

Rind, D.: The sun's role in climate variations, Science, 296, 673–677, 2002.

Rind, D., Lean, J., and Healy, R.: Simulated time-dependent climate response to solar radiative forcing since 1600, J. Geophys. Res., 104, 1973–1990, 1999.

Risebrobakken, B., Jansen, E., Andersson, C., Mjelde, E., and Hevrøy, K.: A high-resolution study of Holocene paleoclimatic and paleoceanographic changes in the Nordic Seas, Paleoceanography, 18, 1017, doi:10.1029/2002PA000764, 2003.

Schaeffer, M., Selten, F. M., and Opsteegh, J. D.: Shifts of means are not a proxy for changes in extreme winter temperatures in climate projections, Clim. Dyn., 25, 51–63, 2005.

Schaeffer, M., Selten, F. M., Opsteegh, J. D., and Goosse, H.: Intrinsic limits to predictability of abrupt regional climate change in IPCC SRES scenarios, Geophys. Res. Lett., 29, 1767, doi:10.1029/2002GL015254, 2002.

Shindell, D. T., Schmidt, G. A., Mann, M. E., Rind, D., and Waple, A.: Solar forcing of regional climate change during the Maunder Minimum, Science, 294, 2149–2152, 2001.

Stuiver, M., Reimer, P. J., Bard, E., Beck, J. W., Burr, G. S., Hughen, K. A., Kromer, B., McCormac, G., Van der Plicht, J., and Spurk, M.: INTCAL98 radiocarbon age calibration, 24 000-0 cal BP, Radiocarbon, 40, 1041–1083, 1998.

van der Schrier, G., Weber, S. L., and Drijfhout, S. S.: Sea level changes in the North Atlantic by solar forcing and internal variability, Clim. Dyn., 19, 435–447, 2002.

van Geel, B. and Renssen, H.: Abrupt climate change around 2650 BP in North-West Europe: evidence for climatic teleconnections and a tentative explanation, in: Water, environment and society in times of climatic change, edited by: Issar, A. S. and Brown, N., Kluwer, Dordrecht, 21–41, 1998.

van Geel, B., Buurman, J., and Waterbolk, H. T.: Archaeological and palaeoecological indications of an abrupt climate change in The Netherlands, and evidence for climatological teleconnections around 2650 BP, J. Quat. Sci., 11, 451–460, 1996.

van Geel, B., van der Plicht, J., Kilian, M. R., Klaver, E. R., Kouwenberg, J. H. M., Renssen, H., Reynaud-Farrera, I., and Waterbolk, H. T.: The sharp rise of ^{14}C around 800 cal BC: possible causes, related climatic teleconnections and the impact on human environments, Radiocarbon, 40, 535–550, 1998.

van Geel, B., Heusser, C. J., Renssen, H., and Schuurmans, C. J. E.: Climate change in Chile at around 2700 BP and global evidence for solar forcing: a hypothesis, Holocene, 10, 659–664, 2000.

Wang, Y. M., Lean, J. L., and Sheeley, N. R.: Modeling the sun's magnetic field and irradiance since 1713, Astrophys. J., 625, 522–538, 2005.

Weber, S. L., Crowley, T. J., and van der Schrier, G.: Solar irradiance forcing of centennial climate variability: linear and nonlinear responses in a coupled model, Clim. Dyn., 22, 539–553, 2004.

Wiersma, A. P. and Renssen, H.: Model-data comparison for the 8.2 ka BP event: confirmation of a forcing mechanism by catastrophic drainage of Laurentide Lakes, Quat. Sci. Rev., 25,

63–88.

Yang, S., Odah, H., and Shaw, J.: Variations in the geomagnetic dipole moment over the last 12 000 years, Geophys. J. Int., 140, 158–162, 2000.

Table 1. Summary of proxy evidence for climate change in period 2800–2600 BP.

Region	Inferred climate change 2800–2600 BP	References
Greenland ice cores (local signal)	No clear signal in site temperature	Masson-Delmotte et al. (2005)
Greenland ice cores (regional signal)	Cold phase, intensified atmospheric circulation	O'Brien et al. (1995)
N Icelandic Shelf	Relatively warm phase /cold phase followed by warming	Andersen et al. (2004); Giraurdeau et al. (2004); Jiang et al. (2002)
Norwegian Sea surface	Distinct cold phase (∼−2°C)	Mikalsen et al. (2001); Andersson et al. (2003); Risebrobakken et al. (2003)
N Europe (Norway)	Cold/dry phase	Nesje et al. (2001)
W Europe (UK, Ireland, France Netherlands)	Widespread cold/wet phase	Magny (1993), van Geel et al. (1996, 1998), Macklin et al. (2003), Holzhauser et al. (2005)
E North America (New England, Michigan)	Wet phase	Brown et al. (2000), Booth et al. (2003)
North Atlantic surface ocean	Changes in surface winds and colder surface ocean	Bond et al. (2001)
North Atlantic deep ocean	Reduced MOC	Bianchi and McCave (1999), Oppo et al. (2003), Hall et al. (2004)
NW Africa	Distinct dry event	Van Geel et al. (1998), Elenga et al. (2004)

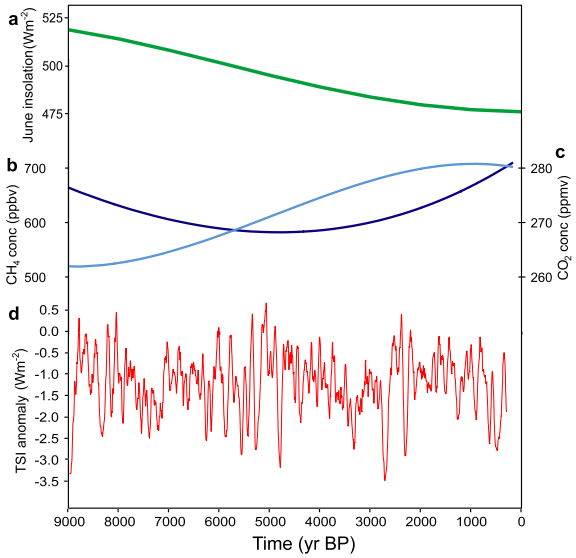

Fig. 1. Forcings applied in the simulation experiments: **(a)** insolation related to orbital forcing (Berger, 1978), shown here is the example of June insolation at 60° N, **(b–c)** smoothed long-term atmospheric concentrations of CH_4 (dark blue, b) and CO_2 (light blue, c) based on ice-core records (Raynaud et al., 2000), and **(d)** TSI anomalies based on ^{14}C (see text).

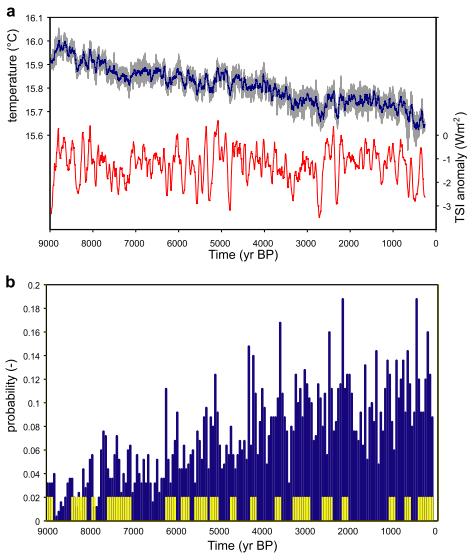

Fig. 2. **(a)** Simulated 5-member ensemble mean annual global surface temperature (25-year running means, left axis) and the ensemble range (in grey) plotted together with TSI anomalies (in red, right axis). **(b)** Probability to have an extremely cold year over Nordic Seas just South of Svalbard (main deep convection area), calculated per 50-year periods. The probability is defined as the occurrences of years with an annual temperature of more than 2 standard deviations below the 9000-year mean in the 5 ensemble members, divided by the total number of years. The long-term cooling trend due to orbital forcing is removed before the analysis by subtracting a linear regression model that was fitted through the annual data. Large TSI anomalies (reaching more than 2 Wm^{-2}) are indicated by yellow bars.

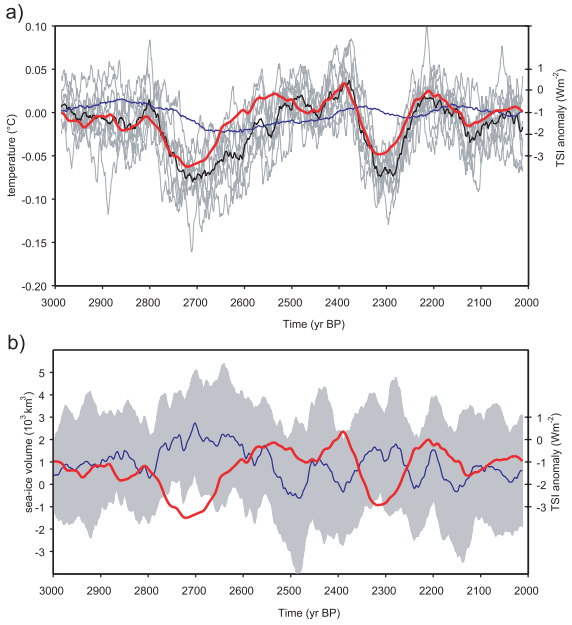

Fig. 3. Simulated 9-member ensemble mean time-series (left axis) together with TSI anomalies (red curves, right axis) for the period 3000–2000 BP: **(a)** global annual atmospheric surface temperature anomaly (25-year running mean, ensemble mean in black, reference period is 3000–2900 BP) with the individual ensemble members shown (in grey) and global ocean temperature (blue), **(b)** annual sea-ice volume in the Northern Hemisphere (25-year running mean, ensemble mean in dark blue) and ±1 standard deviation in grey. The long-term trend is removed (see caption Fig. 2b).

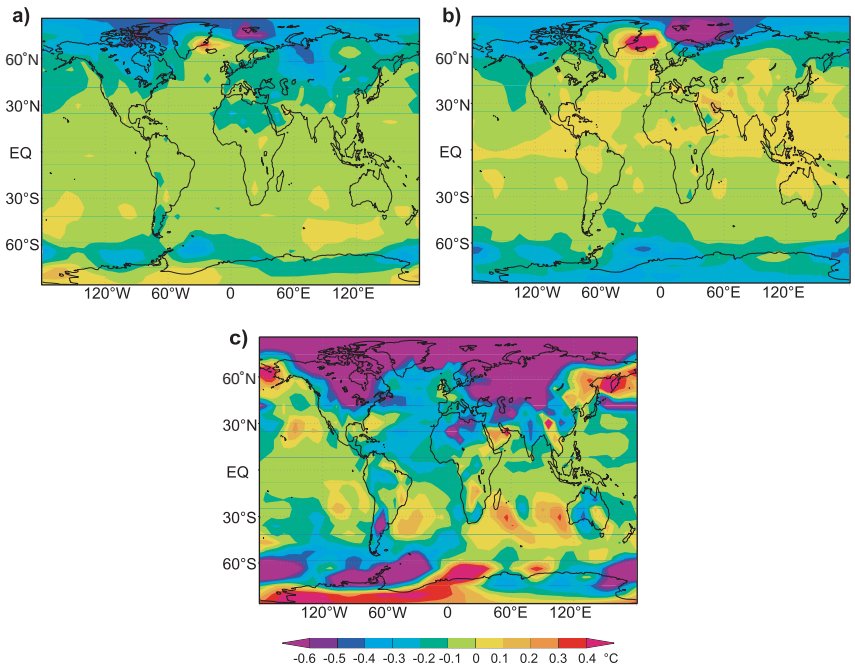

Fig. 4. Simulated annual surface temperature anomaly compared to ensemble mean for 3000–2950 BP (in °C): **(a)** 9-member ensemble mean 2730–2700 BP (maximum TSI reduction), **(b)** 9-member ensemble mean 2650–2600 BP (period when global temperature and TSI diverge), **(c)** coldest decade in one ensemble member.

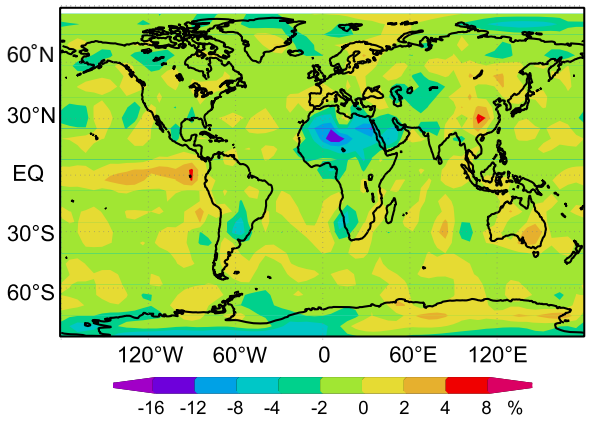

Fig. 5. Simulated 9-member ensemble mean annual precipitation anomaly: 2730–2700 minus 3000–2950 BP (in % of the 3000–2950 BP period). Only the negative anomaly in North Africa (Sahel and parts of Sahara) is statistically significant (i.e., more than the 2-standard deviation level).